Miscibility and Properties of Completely Biodegradable Blends of Poly(propylene carbonate) and Poly(butylene succinate)

M. Z. Pang, J. J. Qiao, J. Jiao, S. J. Wang, M. Xiao, Y. Z. Meng

State Key Laboratory of Optoelectronic Materials and Technologies/Institute of Optoelectronic and Functional Blend Materials, Sun Yat-Sen University, Guangzhou 510275, People's Republic of China

Received 17 October 2006; accepted 27 August 2007
DOI 10.1002/app.27252
Published online 19 November 2007 in Wiley InterScience (www.interscience.wiley.com).

ABSTRACT: Completely biodegradable blends of poly (propylene carbonate) (PPC) and poly(butylene succinate) (PBS) were melt-prepared and then compression-molded. The miscibilities of the two aliphatic polyesters, that is, PPC and PBS, were investigated by dynamic mechanical analysis (DMA) and scanning electron microscopy (SEM). The static mechanical properties, thermal behaviors, crystalline behavior, and melt flowability of the blends were also studied. Static tensile tests showed that the yield strength and the strength at break increased remarkably up to 30.7 and 46.3 MPa, respectively, with the incorporation of PBS. The good ductility of the blends was maintained in view of the large elongation at break. SEM observation revealed a two-phase structure with good interfacial adhesion. The immiscibility of the two components was verified by the two independent glass-transition temperatures obtained from DMA tests. Moreover, thermogravimetric measurements indicated that the thermal decomposition temperatures ($T_{-5\%}$ and $T_{-10\%}$) of the PPC/PBS blends increased dramatically by 30–60°C when compared with PPC matrix. The melt flow indices of the blends showed that the introduction of PBS improved the melt flowability of the blends. The blending of PPC with PBS provided a practical way to develop completely biodegradable blends with applicable comprehensive properties. © 2007 Wiley Periodicals, Inc. J Appl Polym Sci 107: 2854–2860, 2008

Key words: biodegradable; blends; miscibility; polycarbonates

INTRODUCTION

It is well known that the primary factor baffling the development of plastics is the white pollution caused by petroleum-based plastic wastes, especially polyolefins.[1] Aliphatic polyesters exhibit superior biodegradability and good comprehensive properties. Therefore, much attention has been paid to them; they include poly(lactic acid), poly(butylene succinate) (PBS), poly(hydroxybutyrate-*co*-valerate), and polycaprolactone.[2–10] Moreover, the massive emission of CO_2 from industries has been causing serious effects on environment, called *global warming*.[11] The copolymerization of CO_2 with other organic reagents (e.g., epoxide) to form biodegradable aliphatic polycarbonate[12–19] has, therefore, attracted considerable attention in recent years. The use of CO_2 as one of the monomers in the preparation of biodegradable polycarbonate can not only partially get rid of our dependence on petroleum but also provide a new approach to reducing the massive emission of CO_2, which contributes to the greenhouse effect.

Recently, our laboratory successfully synthesized poly(propylene carbonate) (PPC) via the copolymerization of CO_2 with propylene oxide using a supported catalyst.[17–19] By optimizing the reaction conditions, high-molecular-weight PPC with an alternating structure was obtained with high yield (126 g of polymer/g of catalyst). The synthesized PPCs possessed good melt processability and fine biodegradability in surroundings of both soil and buffer solution. However, the PPCs still exhibited poor mechanical properties and thermal stability.

PBS, another biodegradable aliphatic polyester, is known as a crystalline polymer. It possesses superior mechanical properties and excellent thermal stability, which results greatly from its crystalline structure.[2–4] It is well known that the biodegradability of polymers is influenced not only by the chemical structure, especially the presence of functional groups and a hydrophilicity–hydrophobicity balance, but also by a highly ordered structure, such as crystallization, orientation,

Correspondence to: Y. Z. Meng (mengyzh@mail.sysu.edu.cn).

Contract grant sponsor: Natural Science Foundation of China; contract grant number: 50203016.
Contract grant sponsor: Guangdong Province Sci & Tech Bureau; contract grant number: Key Strategic Project 2003C105004.
Contract grant sponsor: Guangzhou Sci & Tech Bureau; contract grant number: 2005U13D2031.

and other morphologies. It has been documented that the amorphous regions are more susceptible to biodegradation than the crystalline regions.[3,20] Therefore, in view of amorphous/crystalline blends (PPC/PBS), the amorphous phase of PPC may promote the biodegradation of these blends.

Blends of PPC reinforced by inorganic or organic fillers, such as $CaCO_3$, SiO_2, montmorillonite, vermiculite, starch, lignocellulose fiber, and wood powder, have been reported.[20–27] These blends generally exhibit superior mechanical strength, stiffness, and heat distortion temperatures with respect to unreinforced polymers. However, because of the agglomeration of fillers during blending, these blends showed poor dispersity, fluidity, and ductility. In this respect, PPCs with another polymeric reinforcement could overcome these problems, such as PPC/PS (OH), PPC/poly(lactic acid), PPC/ethylene-vinyl acetate copolymer (EVA), PPC/poly (hydroxybutyrate-*co*-valerate), PPC/poly(vinyl alcohol) PVA, or PPC/polymethyl methacrylate.[28–34]

In this article, we report on PPC/PBS blends prepared via simple melt blending. The miscibility and the properties of the blends were fully investigated by dynamic mechanical analysis (DMA), scanning electron microscopy (SEM), and other methodologies.

EXPERIMENTAL

Materials

The PPC used in this study was kindly provided by Tian-Guan Enterprise Group Co. (Henan, China) and had a number-average molecular weight (M_n) of 71, 000 and a polydispersity of 3.47. PBS [M_n = 56,000, melting temperature (T_m) = 115°C], with a narrow polydispersity of 1.69, was obtained from Shen-Hua Group (Shanghai, China). PPC and PBS pellets were dried in a vacuum oven for 24 h at 80 and 50°C, respectively.

The PPC/PBS blends with weight ratios of 100/0, 90/10, 70/30, 50/50, 30/70, 10/90, and 0/100 were fabricated in a twin-rotary mixer (Haake Rheomix RT 600, Wehrheim, Germany). The mixing was carried out at 150°C for 10 min at a speed of 30 rpm. For each sample, 50 g of material was fed into the batch. The melt torque values of the blends were recorded during mixing. For the purposes of comparison, neat PPC and PBS resins were also melt-blended under the same processing conditions in the mixer. The mixture was melt-pressed into sheets 1 mm thick and then cut into standard dumbbell tensile bars (ASTM D 638) with dimensions of $25 \times 4 \times 1$ mm^3.

Characterization

The static tensile tests were performed at 23°C with a relative humidity of 50 ± 5% with a tensile tester (New SANS, Shenzhen, China). The crosshead speed was set at 25 mm/min. Five specimens of each sample were tested, and the average results were recorded. Before the measurements, the specimens were conditioned at 23°C and 50 ± 5% humidity for 24 h by their placement in a closed chamber containing a saturated $Ca(NO_3)_2 \cdot 24H_2O$ solution in distilled water (ASTM E 104).

DMA was carried out with a DuPont DMA instrument (model 983) (Wilmington, DE) at a fixed frequency of 1 Hz and an oscillation amplitude of 0.2 mm. The dimensions of the specimens were $30 \times 10 \times 1$ mm^3. The scanning temperature ranged from −80 to 80°C at a heating rate of 2°C/min.

The samples were scanned with differential scanning calorimetry (DSC; Netzsch 204, Burlington, Germany). To remove the previous thermal and stress history of the samples, they were initially scanned to 150°C with a heating rate of 10°C/min, maintained at this temperature for 5 min, and then quenched to −80°C with the same heating rate and remaining for another 5 min. The samples were subsequently rescanned from −80 to 150°C at a heating rate of 10°C/min. All the scanning processes were under a protective atmosphere of N_2.

Thermogravimetric (TG) measurements were conducted on a PerkinElmer TGA-6 instrument (Yokohama, Japan) under a N_2 protective atmosphere. The scanning temperature ranged from 30 to 500°C with a heating rate of 20°C/min.

Wide-angle X-ray diffraction (WAXD) measurements were performed with an X-ray diffractometer (D/Max-IIIA, Rigaku, Japan) at a scanning speed of 5°/min with a 2θ ranging from 5–40°. The X-ray source was a 3-kW rotating anode X-ray generator equipped with a rotating anode Cu target.

Melt flow indices (MFIs) of the blends with various weight ratios were examined with a MFI instrument (MC-400C, Taiwan, China) equipped with a standard die. The die had a smooth straight bore with a diameter of 2.0955 ± 0.0051 mm and a length of 8.000 ± 0.025 mm. The measurements were performed according to ASTM D 1238-82. The melt-extrusion temperature ranged from 150 to 180°C. Different loads (1.20, 2.16, 3.80, and 5.00 kg) were used to study the melt flowability of the blends under different conditions.

Fourier transform infrared (FTIR) spectra were taken on an FTIR-100 spectrometer (PerkinElmer). The blends were first hot-pressed to a thin film and then examined with wave numbers from 4000 to 400 cm^{-1}.

The PPC/PBS blend specimens were fractured in liquid nitrogen, and then, the fracture surfaces were coated with a thin layer of gold. A scanning electron microscope (Jeol JSM-6330F) was used to observe the micromorphology of the blends.

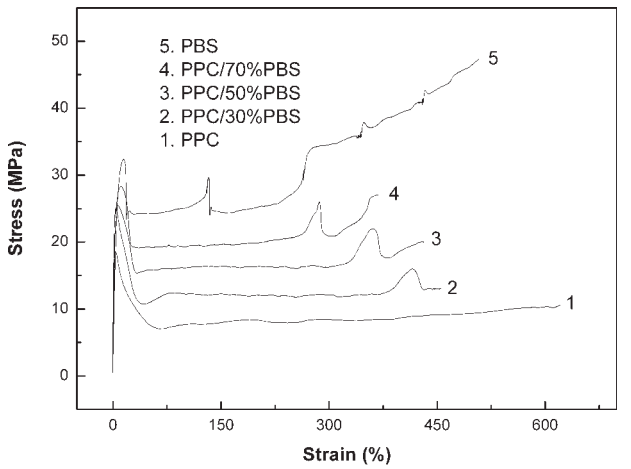

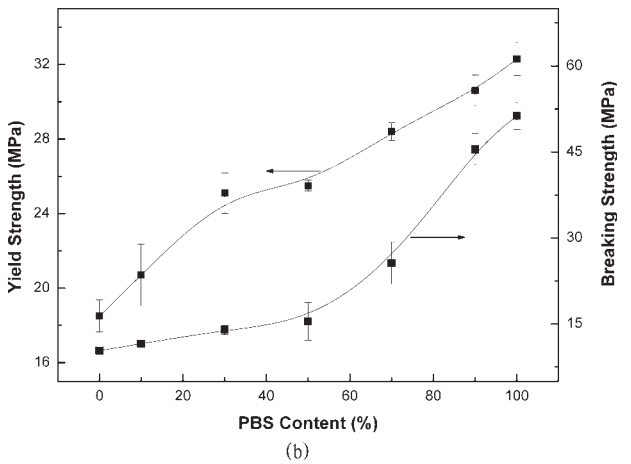

Figure 1 Tensile properties for neat PPC and PBS and the PPC/PBS blends: (a) stress–strain curves and (b) yield strength and breaking strength versus PBS content.

RESULTS AND DISCUSSION

Static and dynamic mechanical properties

Tensile properties for neat PPC and PBS and the PPC/PBS blends are shown in Figure 1. PPC is a ductile polymer with lower yield strength and strength at break. With the addition of PBS, both the yield strength and breaking strength increased remarkably. However, the elongation at break had no sharp contraction, which indicated that good ductility was maintained. Under external stress, orientation or yield was observed. In Figure 1(a), several small sharp peaks, which we called *secondary yield,* were observed, which resulted from the multiple segment orientations during the tensile process. After each secondary yield, the stress of the blends increased further. The strength at break of neat PBS even increased up to 51.3 MPa with several secondary yields.

As shown in Figure 1(b), both the yield strength and the strength at break increased with increasing PBS content. When the PBS content was less than 50%, the yield strength of the blends was augmented dramatically due to the orientation-strengthening effect of the PBS content. However, the strength at break seemed to be more dependent on the corresponding continuous phase. The strength at break of the blends increased relatively slowly when the PBS content was lower than 70%. For the PPC/90% PBS blends and neat PBS, the strength at break was much higher than the corresponding yield strength. Moreover, the elongation at break of the PPC/PBS blends decreased slightly followed by an increase with further increasing PBS content. All elongations at break remained at large values, which demonstrated the good ductility of the blends.

To investigate the miscibility between PPC and PBS, DMA of the blends was performed. As shown in Figure 2, sharp changes in storage modulus (E'), loss modulus (E''), and tan δ at the glass-transition temperature (T_g) were observed. Two independent T_g's (Fig. 2) indicated the immiscibility between PPC and PBS.

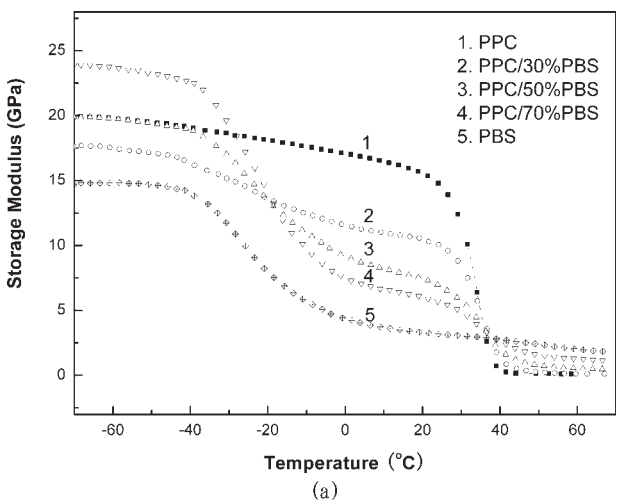

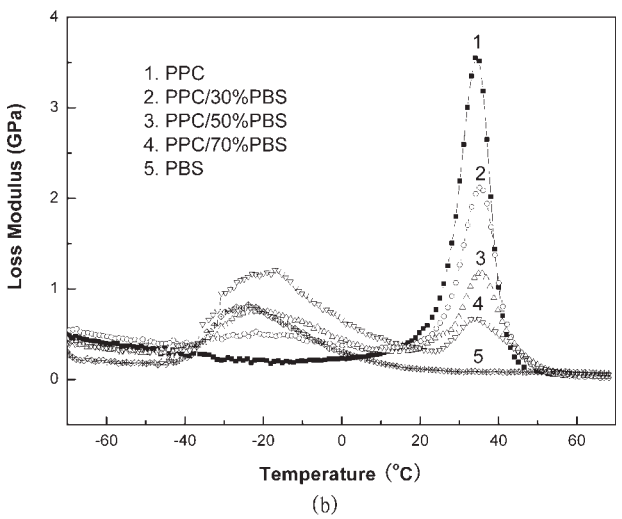

Figure 2 DMA curves for neat PPC and PBS and the PPC/PBS blends: (a) E' versus temperature and (b) E'' versus temperature.

TABLE I
T_g Values of the Two Phases for the PPC/PBS Blends Obtained from Figure 2(b)

Sample	T_g^1 (°C)	T_g^2 (°C)	ΔT_g (°C)
PPC	—	34.4	—
PPC/30% PBS	−21.9	35.2	57.1
PPC/50% PBS	−21.6	35.1	56.7
PPC/70% PBS	−17.9	34.4	52.3
PBS	−24.3	—	—
ΔT_g^0 (°C)	$T_g^{PPC} - T_g^{PBS}$		58.7

ΔT_g, the *D*-value of the two glass-transition temperatures for the two phase blends; ΔT_g^0, the *D*-value of the two glass-transition temperatures for the two resins without blending; T_g^{PPC} and T_g^{PBS}, the glass transition temperature of PPC resin and PBC resin, respectively.

As shown in Figure 2(b), we could easily obtain the glass-transition temperature of the PBS-rich phase (T_g^1) and the glass-transition temperature of the PPC-rich phase (T_g^2) for the PPC/PBS blends. The *D* values, that is, ΔT_g, were calculated by the subtraction of T_g^2 and T_g^1. ΔT_g^0 was denoted as $T_g^{PPC} - T_g^{PBS}$; the value was 58.7°C. The results are listed in Table I. Apparently, the smaller the value of ΔT_g was, the better the miscibility between the two phases was. As shown in Table I, the miscibility of PPC and PBS was improved with increasing PBS content. This partially resulted from the fact that PBS gradually appeared to become the continuous phase due to its lower melt viscosity.

Thermal properties of the PPC/PBS blends

The understanding of nonisothermal crystallization behavior is of great importance because most processing techniques are actually conducted under nonisothermal conditions. The crystallinity (X_c) of PBS with different PBS contents could be calculated from the following formula:

$$X_c = (\Delta H_c / \Delta H_0) \times 100\% \quad (1)$$

where ΔH_c is the heat of crystallization and is calculated from the exothermal peak area in DSC curves and ΔH_0 is the exothermal heat when X_c is 100%.

TABLE II
Characteristic Values of the DSC Curves for Neat PPC and PBS and the PPC/PBS Composites

Sample	T_c (°C)	ΔH_c (J/g)	T_m (°C)	ΔH_f (J/g)
PPC	/	/	/	/
PPC/10% PBS	/	/	103.2	3.84
PPC/30% PBS	70.7	11.3	115.5	19.6
PPC/50% PBS	72.4	30.7	115.2	36.7
PPC/70% PBS	71.8	44.3	115.7	52.0
PPC/90% PBS	65.0	51.1	114.6	64.7
PBS	69.6	65.7	115.5	75.5

Figure 3 shows the endothermic peaks that corresponded to the fusion of the PBS phase. With increasing PBS content, X_c, the heat of fusion (ΔH_f), and ΔH_c of the blends increased obviously, although when the PBS content was higher than 50%, there was an exothermic peak before the main endothermic peak. Presumably, this resulted from the fusion and recrystallization of PBS crystallites during heating.[2,35]

Table II lists the values of the crystallization temperature (T_c), ΔH_c, T_m, and ΔH_f. For the PPC/PBS blends with a PPC content higher than 10%, the nonisothermal T_c was higher than that of neat PBS, which implied that PPC acted as a nucleation agent for the PBS phase. Meanwhile, T_m of neat PBS was higher than those of the PPC/PBS blends. This suggested that the reduction in PBS ΔH or PBS X_c was correlated to the interaction between the two components to some extent.

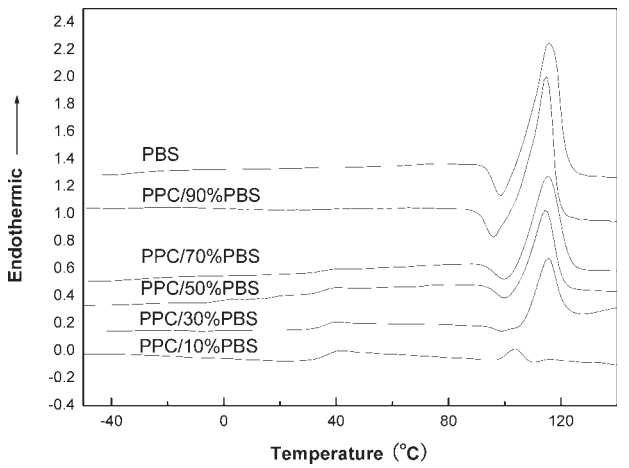

Figure 3 DSC curves of neat PBS and the PPC/PBS blends.

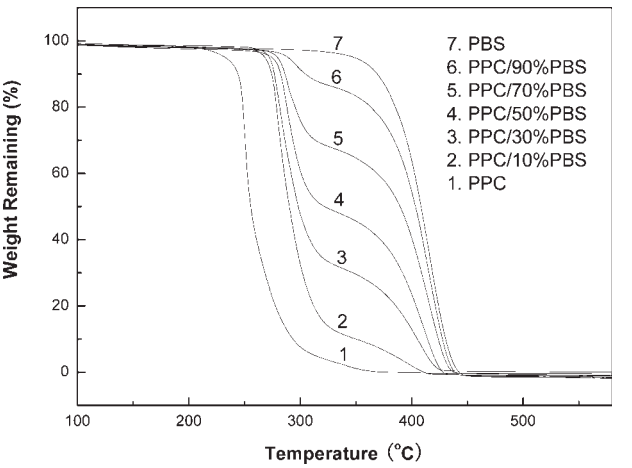

Figure 4 TG curves for neat PPC and PBS and the PPC/PBS blends.

TABLE III
Thermal Stabilities of Neat PPC and PBS and the PPC/PBS Blends

Sample	$T_{-5\%}$ (°C)	$T_{-10\%}$ (°C)	T^1_{max} (°C)	T^2_{max} (°C)
PPC	232.6	244.1	253.1	—
PPC/10% PBS	268.3	274.3	283.5	398.0
PPC/30% PBS	272.2	276.7	285.5	410.9
PPC/50% PBS	274.9	282.3	291.4	412.0
PPC/70% PBS	279.7	286.2	289.8	418.6
PPC/90% PBS	289.3	304.5	298.1	418.3
PBS	348.5	369.1	—	419.9

T^1_{max} and T^2_{max} were denoted as the thermal decomposition temperature with the max rate of the PBS-rich phase and PPC-rich phase, respectively.

The TG curves of neat PPC and PBS and the PPC/PBS blends are shown in Figure 4. The corresponding characteristic temperatures are given in Table III. The thermal decomposition temperatures ($T_{-5\%}$ and $T_{-10\%}$) of the PPC/PBS blends increased dramatically by 30–60°C compared with that of the PPC matrix. Both 5% weight loss temperature and maximum weight loss temperature showed that the thermal stability of PPC could be greatly improved by the incorporation of a small amount of PBS.

WAXD examination

It has been documented that amorphous regions are more susceptible to biodegradation than crystalline regions. Therefore, X_c and the crystalline morphologies are major rate-determining factors of the biodegradability of polymers.[3,16] For the completely biodegradable PPC/PBS blends, we controlled or altered the biodegradable rate by simply changing the ratio of the components.

Figure 5 shows the X-ray diffraction curves of the PPC/PBS blends. A weak peak and a shoulder peak originating from the PBS crystallites were observed for PBS-rich blends. The diffraction peaks at 19.7, 22.0, 22.9, and 29.3° corresponded to the PBS crystalline planes (020), (021), (110), and (111), respectively.[2] However, for the PPC-rich blends, there were only two weak diffraction peaks at 19.7 and 22.9°. Therefore, the crystalline morphology of PBS was influenced by PPC to some extent.

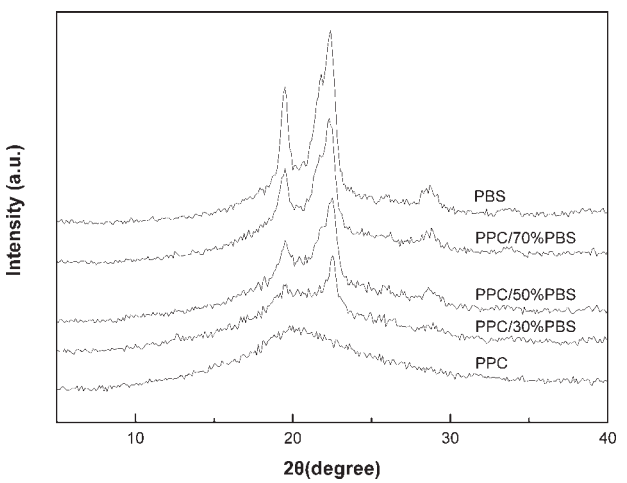

Figure 5 WAXD patterns for neat PPC and PBS and the PPC/PBS blends.

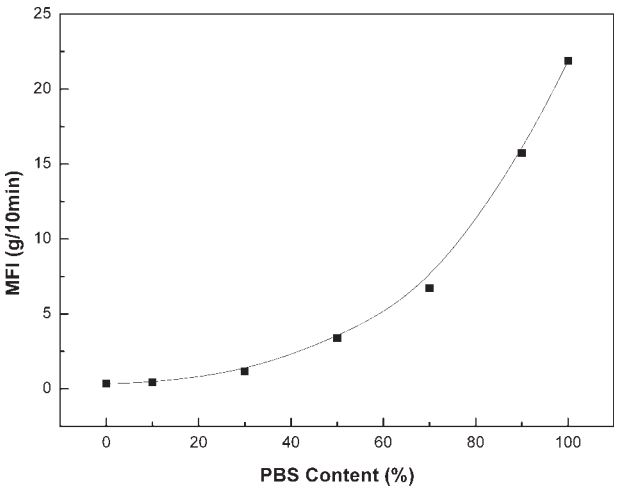

Figure 6 MFI versus PBS content for neat PPC and PBS and the PPC/PBS blends (load: 2.160 kg; temperature: 150°C).

MFI measurements

The MFIs of neat PPC and PBS and the PPC/PBS blends were determined, and the results are shown in Figure 6. Generally, crystalline polymers have lower melt viscosities compared with amorphous polymers. Therefore, the MFIs of the PPC/PBS blends increased with increasing PBS content.

Figure 7 shows the MFIs of PPC/30% PBS obtained under different loads and different temperatures. As expected, the MFI increased with increasing load and temperature.

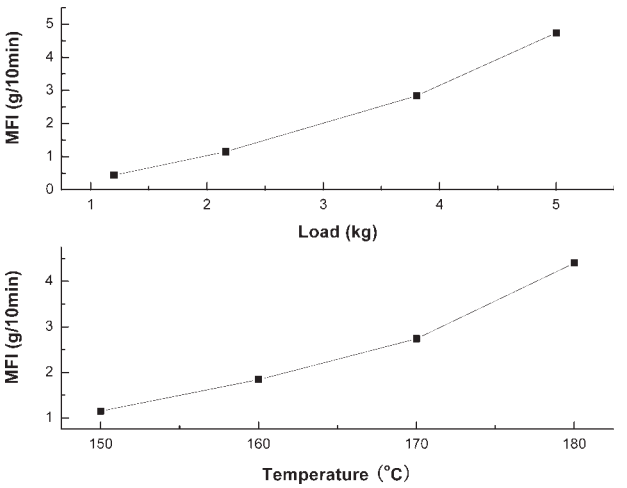

Figure 7 MFI versus load and temperature for the PPC/30% PBS blend.

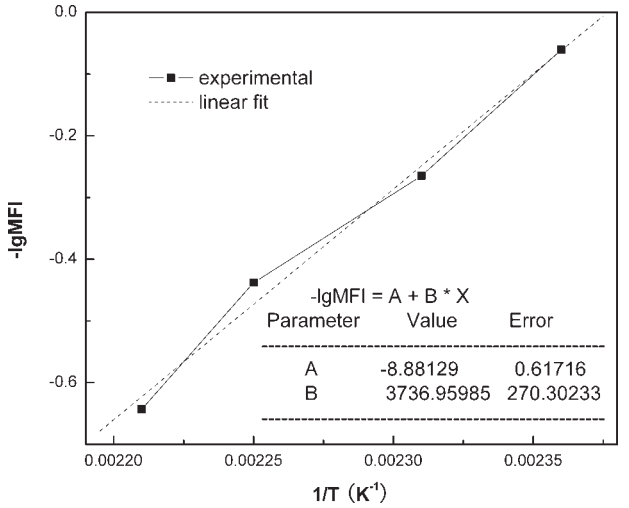

Figure 8 −Log MFI versus $1/T$ for the PPC/30% PBS blend.

According to the Andrade equation and the Poiseuille equation, the relationship between MFI and the flow activation energy (E_η) can be given as follows:[36]

$$-\log \mathrm{MFI} = A + E_\eta/2.303\,RT \qquad (2)$$

where R is the universal constant, T is the temperature and A is a constant. A linear relationship between −log MFI and $1/T$ is shown in Figure 8. From the linear fitting of the curve, we obtained the value of the intercept (A) and the slope (B) of the line. Finally, E_η of the PPC/30% PBS blend was found to be 71.56 kJ/mol.

FTIR spectra

To explore possible interactions between PPC and PBS accordingly, we ran a FTIR analysis of the PPC/PBS composites. As shown in Figure 9, the peaks at 1750 cm^{-1} (C=O) and 1250 cm^{-1} (C—O) became broader with increasing PBS content with respect to those of the neat PPC and PBS resins. This was probably due to the interactions between the C=O or C—O and the O—H of the chain ends of both PPC and PBS. This was also observed from the peaks at

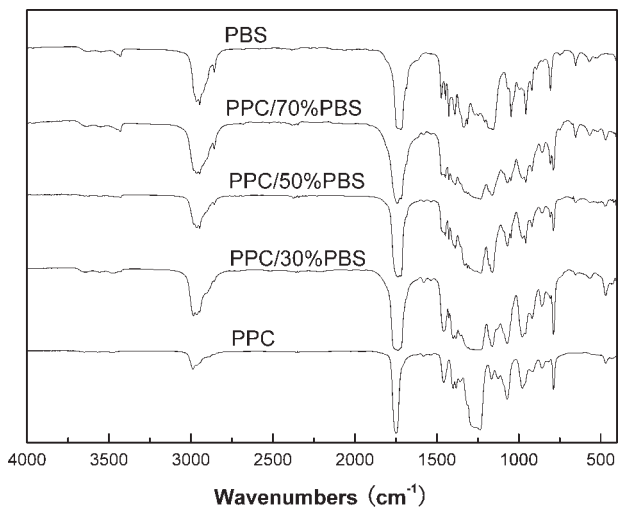

Figure 9 FTIR spectra of neat PPC and PBS and the PPC/PBS blends.

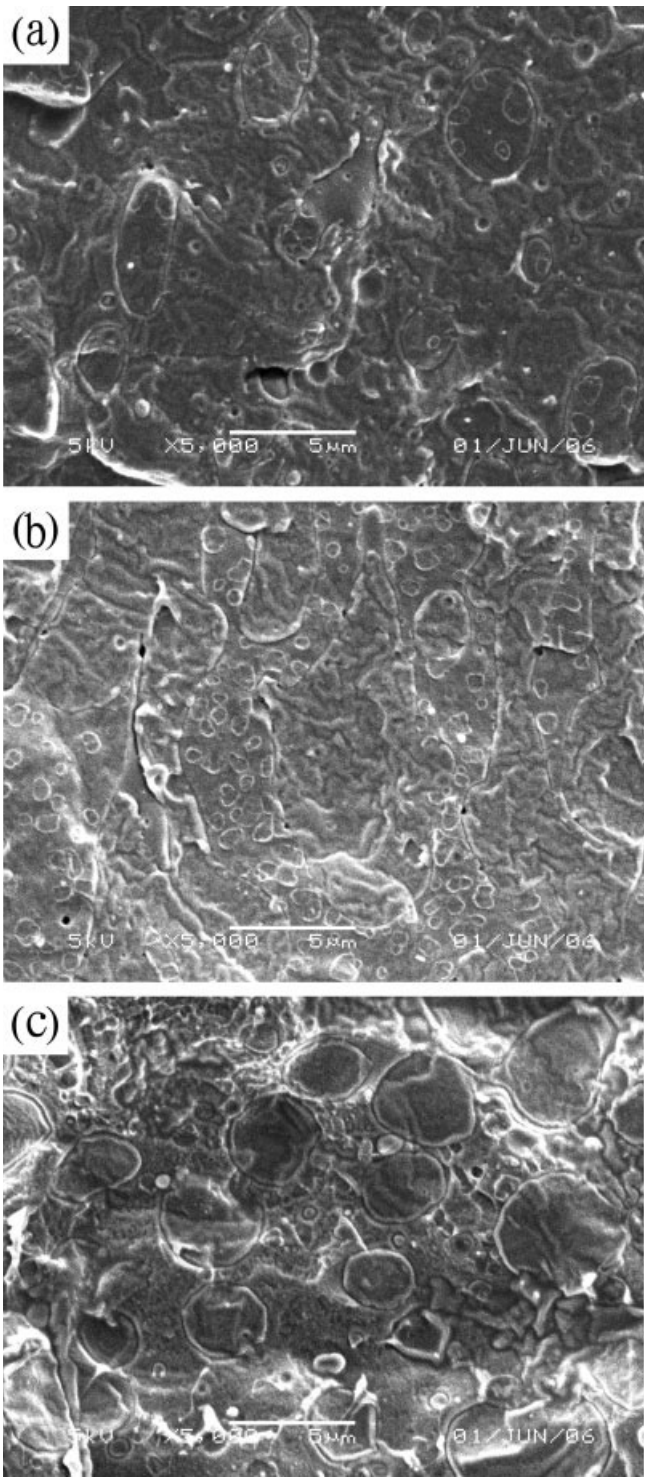

Figure 10 SEM photos for the PPC/PBS blends: (a) PPC/30% PBS, (b) PPC/50% PBS, and (c) PPC/70% PBS.

4000–3500 cm^{-1} (O—H). These interactions were believed to contribute to the improved mechanical and thermal properties of the blends.

Morphology observations

The SEM micrographs of the cross-section surface of the PPC/PBS blends are shown in Figure 10. A two-phase microstructure was observed with an explicit interface between the two phases. When the content of the dispersed phase was less than 50%, it dispersed well within the continuous phase in the shape of approximately spherical particles. This was termed a *sea-island structure.* The size of dispersed spherical particles tended to increase with increasing the content of the dispersed phase. When the PBS content ranged from 30 to 50%, a transition composition was observed from the continuous PPC phase to the continuous PBS phase. In this case, the mechanical properties of PPC/PBS fit the rule of a typical two-phase blend.

CONCLUSIONS

PPC can be simply melt-blended with PBS to produce completely biodegradable blends with satisfactorily comprehensive properties. Both the yield strength and strength at break of the blends increased with increasing PBS content, together with good ductility. DMA tests showed the immiscibility between the PPC and PBS phases. A basic two-phase microstructure was observed from the SEM micrographs of the blends. T_c of the PBS phase was increased by the incorporation of the PPC phase, which led to a decrease in X_c of the PBS phase. The thermal stability of PPC was greatly improved by the introduction of the PBS phase, as disclosed by TG measurements. MFIs of the blends revealed that the melt flowability was also improved by the blending of PPC with PBS. The improved comprehensive properties of the PPC/PBS blends will provide them with wide application as completely biodegradable blends.

References

1. Bugoni, L.; Krause, L.; Virginia, P. M. Mar Pollut Bull 2001, 42, 1330.
2. Jun, W. P.; Seung, S. I. J Appl Polym Sci 2002, 86, 647.
3. Young, J. K.; Park, O. O. J Environ Polym Degrad 1999, 7, 53.
4. Tsutomu, O.; Lee, S. H. J Appl Polym Sci 2005, 97, 1107.
5. Arvanitoyannis, I. J Macromol Sci Rev Macromol Chem Phys 1999, 39, 205.
6. Qiu, Z. B.; Ikehara, T.; Nishi, T. Polymer 2003, 44, 7519.
7. Eastmond, G. C. Adv Polym Sci 1999, 149, 59.
8. Arvanitoyannis, I. J Macromol Sci Rev Macromol Chem Phys 1999, 39, 205.
9. Gupta, A. P.; Kumar, V. Eur Polym J 2007, 43, 4053.
10. Gupta, B.; Revagade, N.; Hilborn, J. Prog Polym Sci 2007, 32, 455.
11. Meehl, G. A.; Washington, W. M. Nature 1996, 382, 56.
12. Inoue, S.; Koinuma, H.; Tsurata, T. J Polym Sci Polym Lett Ed 1969, 7, 287.
13. Ree, M.; Hwang, Y. T.; Kim, H. Polym Prepr 2000, 41, 1859.
14. Ma, X.; Yu, J.; Zhao, A. Compos Sci Technol 2006, 66, 2360.
15. Xie, Z. G.; Guan, H. L.; Chen, L.; Tian, H. Y.; Chen, X. S.; Jing, X. B. Polymer 2005, 46, 10523.
16. Guan, H. L.; Xie, Z. G.; Tang, Z. H.; Xu, X. Y.; Chen, X. S.; Jing, X. B. Polymer 2005, 46, 2817.
17. Meng, Y. Z.; Du, L. C.; Tjong, S. C.; Zhu, Q.; Hay, A. S. J Polym Sci Part A: Polym Chem 2002, 40, 3579.
18. Wang, S. J.; Tjong, S. C.; Du, L. C.; Zhao, X. S.; Meng, Y. Z. J Appl Polym Sci 2002, 85, 2327.
19. Zhu, Q.; Meng, Y. Z.; Tjong, S. C.; Zhao, X. S.; Chen, Y. L. Polym Int 2002, 51, 1079.
20. Li, X. H.; Tjong, S. C.; Meng, Y. Z.; Zhu, Q. J Polym Sci Part B: Polym Phys 2003, 41, 1806.
21. Mochizuki, M.; Hirami, M. Polym Adv Tech 1997, 8, 203.
22. Ge, X. C.; Li, X. H.; et al. Polym Eng Sci 2004, 44, 2134.
23. Li, X. H.; Meng, Y. Z.; Zhu, Q.; Rajula, A. V.; Tjong, S. C. J Polym Sci Part B: Polym Phys 2004, 42, 666.
24. Ge, X. C.; Zhu, Q.; Meng, Y. Z. J Appl Polym Sci 2006, 99, 782.
25. Ge, X. C.; Xu, Y.; Meng, Y. Z.; Li, R. K. Y. Compos Sci Technol 2005, 65, 2219.
26. Xu, J.; Li, R. K. Y.; Meng, Y. Z.; et al. Mater Res Bull 2006, 41, 244.
27. Xu, J.; Li, R. K. Y.; Xu, Y.; Meng, Y. Z. Eur Polym J 2005, 41, 881.
28. Qiu, F. R.; Chen, S. M.; Tan, L.; Ping, Z. H. Polymer 2004, 45, 3045.
29. Wang, X. L.; Du, F. G.; Meng, Y. Z.; Li, R. K. Y. Mater Lett 2006, 60, 509.
30. Zhang, Z. H.; Zhang, H. L.; Zhang, Q. X. J Appl Polym Sci 2006, 100, 584.
31. Ma, X. F.; Yu, J. G.; Wang, N. J Polym Sci Part B: Polym Phys 2005, 44, 94.
32. Li, J.; Lai, M. F.; Liu, J. J. J Appl Polym Sci 2005, 98, 1427.
33. Obeson, L. M.; Kuphal, J. A. U.S. Pat. 4,912,149 (1990).
34. Kuphal, J. A.; Robesoa, M.; Weber, J. J. U.S. Pat. 4,874,030 (1989).
35. Lai, S. M.; Huang, C. K.; Shen, H. F . J Appl Polym Sci 2005, 97, 257.
36. Saini, D. R.; Shenoy, A. V. J Macromol Sci Phys 1983, 22, 437.